CTURE

e Effects on the Mixed-Mode Delamination
tion and Debonding of Materials, ASTM
'esting and Materials, Philadelphia, 1985,

"Effect of Matrix Resin on Delamination
ring Fracture Mechanics, Vol. 49, 1994,

Assimina A. Pelegri,[1] *George A. Kardomateas,*[1]
and Basharat U. Malik[1]

The Fatigue Growth of Internal Delaminations Under Compressive Loading of Cross-Ply Composite Plates

REFERENCE: Pelegri, A. A., Kardomateas, G. A., and Malik, B. U., **"The Fatigue Growth of Internal Delaminations Under Compressive Loading of Cross-Ply Composite Plates,"** *Composite Materials: Fatigue and Fracture (Sixth Volume), ASTM STP 1285*, E. A. Armanios, Ed., American Society for Testing and Materials, 1997, pp. 143–161.

ABSTRACT: This study focuses on the mode dependence of delamination growth under cyclic compressive loads in cross-ply composite plates. The model proposed makes use of an initial postbuckling solution derived from a perturbation procedure. A mode-dependent crack growth criterion is introduced. Expressions describing the fatigue crack growth are derived in terms of the distribution of the mode adjusted energy release rate. The resulting crack growth laws are numerically integrated to produce delamination growth versus number of cycles diagrams. The model does not impose any restrictive assumptions on the relative thickness of the delaminated and the base plates, although transverse shear stress effects are not considered. Experimental results are presented for cross-ply graphite/epoxy specimens, and the results are compared with experimental results for unidirectional specimens. The test data are obtained for different delamination locations and for different values of applied compressive strain.

KEYWORDS: composite materials, fatigue (materials), delamination, energy release rate, mode mixity, stress intensity factor, crack growth law, fracture (materials)

The applicability of laminated composite materials may become limited due to the frequent presence of delaminations, that is, partial debonding of the plies of the laminate. This partial debonding at the interface is most commonly a result of manufacturing imperfections, low velocity impacts on the surface of the composite component, or even a consequence of vibrations of the structure's propulsion system. The effect of the delamination growth can be manifested in the form of stiffness and strength degradation as well as a change in the energy absorption capacity of composite beam structures [*1,2*].

The study of the delamination buckling under compression in composite plates has attracted a substantial number of researchers who have studied extensively one-dimensional and two-dimensional configurations [*3–7*]. However, most of this work is concerned with the estimation of the bifurcation point and little attention is paid to the study of the postbuckling behavior of the composite structure. Furthermore, most investigations are focused on theoretical aspects in the absence of experimental studies especially on fatigue loading; some experimental studies have been focused on monotonic (static) loading [*8*].

[1]Graduate research assistant, associate professor, and graduate research assistant, respectively, School of Aerospace Engineering, Georgia Institute of Technology, Atlanta, GA 30332-0150.

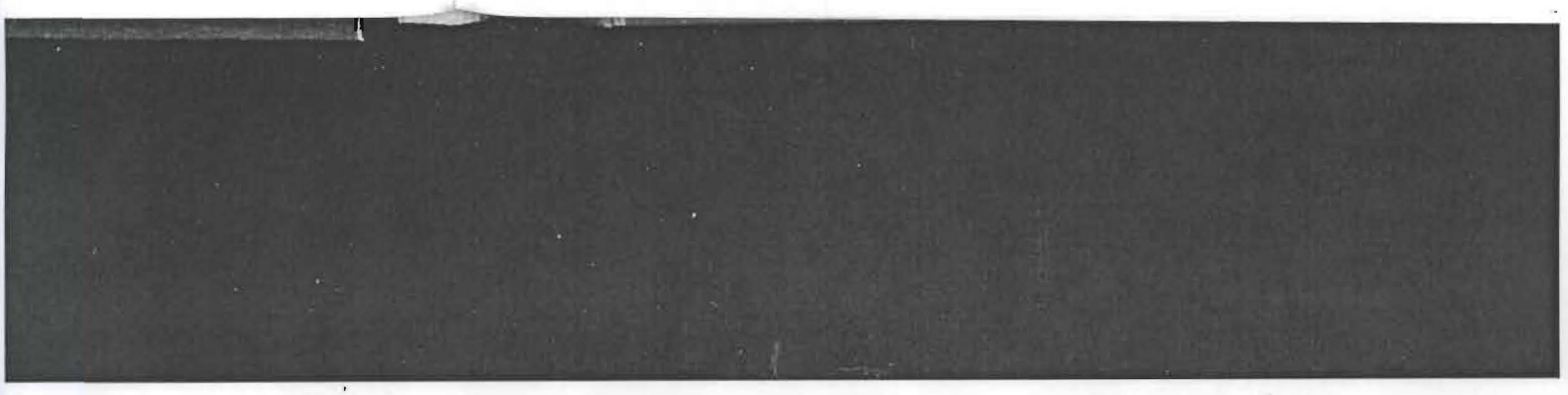

The cyclic loading of delaminated plates has been studied separately under the light of pure Mode I and pure Mode II fatigue loading [*9,10*] and a few studies refer to mode-dependent cyclic delamination growth [*11*]. During the compressive fatigue loading, the delaminated layer undergoes sequential buckled/unbuckled geometrical configurations, as the composite structure is loaded and unloaded, respectively. The repeated cyclic loading of the structure results in the decrease of the material's interlayer resistance. As a consequence, there is damage accumulation in front of the crack-tip that might lead to growth and even potential loss of structural integrity.

The characteristics of delamination growth behavior beyond the bifurcation point can be determined once a postbuckling solution is available. The post critical behavior of delaminations of arbitrary size has been investigated in Refs *12* and *13*. The result of these studies was an analytical formulation for the initial postbuckling behavior, using the theory of elastica to represent the deflections of the buckled layer. This work resulted in a system of nonlinear equations. This model was further developed into a closed-form solution using a perturbation procedure based on the asymptotic expansion of the load and deformation quantities in terms of the distortion parameter of the delaminated layer. This analysis led to closed-form expressions for the force and moment quantities near the crack-tip field in terms of the applied compressive displacement.

The growth characteristics of a postbuckled delaminated composite structure is of major concern. To this extent, we are interested in whether the delamination grows in a stable or unstable manner and, if the growth is stable, the growth rate. These growth characteristics can be investigated once a postbuckling solution is available. The stability of laminated structures is sensitive to the in-plane dimensions (for example, delamination length), the flexural and in-plane stiffnesses, and the loading conditions [*14–18*]. Kardomateas and Pelegri [*16*] investigated the effect of the applied strain and the delamination length on the stability of the delamination growth. Combinations of delamination length and applied strain inducing unstable growth were examined. Comparing the results with the "thin film" model [*3*], one concludes that the delamination growth is more likely to be stable than predicted by this model.

A mode-dependent crack growth law is developed by using the bi-material interface crack solutions for the mode mixity and the energy release rate. For a buckled configuration in compressed films, Evans and Hutchinson [*5*] derived a formula for the energy release rate using an asymptotically valid solution. Yin calculated the energy release rate for a circular delamination using a path independent integral approach [*19*]. In the present study, the energy release rate at the delamination tip is derived in closed-form through a perturbation analysis in the initial postbuckling phase.

Another aspect of delamination growth is the mode dependence of the growth process. Delaminations in composites are interlaminar cracks that are constrained to move in a specific plane (along the layer interface). Therefore, delaminations grow under mixed-mode conditions, that is, a combination of Mode I (opening mode) and Mode II (shearing mode). Traditionally, the growth behavior of delaminations was studied by using the Irwin-Griffith concept of critical fracture energy, utilizing a mode independent energy release rate criterion. Recent experimental studies on several composite materials have shown the inadequacy of mode-independent models [*20,21*]. In this study, a fatigue growth mode-dependent law introduced by Kardomateas et al. in Ref *11* constitutes the basis for the research presented in this paper.

Specifically in this study, Kardomateas et al. [*11*] examined the fatigue growth of delaminations under constant amplitude compressive loads for unidirectional graphite/epoxy plate specimens. This investigation is extended herewith by studying cross-ply construction of graphite/epoxy specimens, again under constant amplitude cyclic compression. The structure is analyzed by being separated into three different parts, that is, the delaminated, substrate, and base parts. The analytical model was proposed for isotropic material by Kardomateas [*12*]

and has been modified to accommodate cross-ply composite models. Although the model does not include classical laminate theory, for example, Refs *22* and *23*, in order to account for layup variations, the rule of mixtures is used in order to account for the material properties in each different part. This approach is being adopted in order to reduce calculation complexity in the initial postbuckling solution. Since the focal point of the study is to examine the trends that exist in various parameters during delamination growth and to correlate analytical and experimental results, the aforementioned analysis is justified. The model utilizes the elastica theory [*24*] by considering all three plates in each configuration as parts of three different compressive elasticae. During the perturbation procedure, the loading and geometric quantities are asymptotically expanded in terms of the distortion parameter of the delaminated plate. The analysis results in closed-form solutions for the applied load and the near tip resultant moments and forces as a function of the applied compressive displacement. Next, the interface crack solutions, as given in Refs *25* and *26*, are employed for the mode mixity and the energy release rate in terms of the resultant moments and forces. The mode-dependent cyclic growth law was employed and correlated with experimental results. Finally, the dependence of the energy release rate and the mode mixity on the delamination growth is examined. The results extracted for the unidirectional graphite/epoxy plate are compared with cross-ply configurations of the same material.

Theoretical Analysis

Postbuckling Solution for a Delaminated Beam/Plate

A delaminated composite structure can be considered an aggregate of three parts, as in Fig. 1. The first part of the thickness, h, consists of the plies laying above the delamination and is referred to as the "delaminated part." The second part of the thickness, $H = T - h$, consists of the plies laying below the delamination and is referred to as the "substrate part." The remaining intact laminate of the thickness, T, is the "base plate." Without loss of generality, it may be assumed that $h < T/2$. The length of the structure is $2L$, and the initial length of

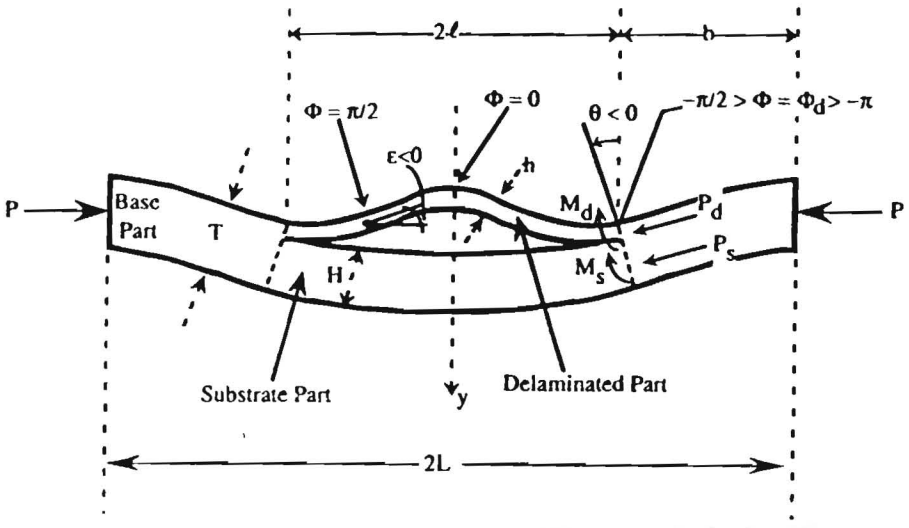

FIG. 1—*Model configuration in the post-buckled state under compressive loading. The delamination separates the configuration into the delaminated, substrate and base plates.*

the delamination is 2ℓ. The delamination is positioned symmetrically along the length of the specimen. The length of the base plate is b, where $b = L - \ell$. The subscript, $i = d, s, b$, refers to the delaminated part, the substrate part, and the base plate, respectively. The material is considered to be linearly elastic and orthotropic.

For the general case of a delaminated composite system, the initial postbuckling solution was studied by Kardomateas [*12*] and led to a closed-form solution. The results produced by this model applied to a unidirectional composite plate were presented in Ref *11*. In the present study, the material layup is $[(0/90)_{14}, 0]$ and $[(0/90)_{28}, 0]$. In addition, due to the complexity of calculations in the initial postbuckling solution, the delaminated plate is considered to be a laminate with averaged material properties determined by the rule of mixtures [*27*]. Similar assumptions are made for the substrate and the base plates. The averaged composite Young's modulus, E, is the corresponding primary composite modulus of elasticity, as defined in Agarwal [*27*], and is valid when the fibers are intact. The bending stiffness of each corresponding plate is denoted by D_i, $D_i = E_i t_i^2/[12(1 - \nu_{12}\nu_{21})]$, where t_i is the thickness of the i^{th} plate, ν_{12} is the Poisson's ratio in the longitudinal direction, and ν_{21} is the Poisson's ratio in the transverse direction of the material. A brief description for the initial postbuckling solution is presented, and the closed-form solution derived will be used to determine the characteristics of the cyclic growth.

The theory of elastica [*24*], provides the exact laws that govern the behavior of single compressive elements elastically restrained at the ends by means of concentrated forces and moments. The generalized coordinates of deformation are the distortion parameter, α_i (where $i = d, s, b$ for the delaminated, substrate, and base plates, respectively), that represents the tangent rotation of each individual plate at an inflection point from the straight position, and the amplitude variable, $\Phi(x)$. The deformations from the initial postbuckling configuration are assumed to be relatively small. The expressions describing the model are expanded in Taylor series in terms of the distortion parameter of the delaminated plate, α_d. For the initial postbuckling solution, a perturbation analysis is utilized with a perturbation parameter, ϵ, such that $\epsilon = \alpha_d$.

Consider the configuration shown in Fig. 1. The model assumes that the buckled delaminated plate is a part of an inflectional elastica with an amplitude, Φ_d, and a distortion parameter, α_d. At the critical state, the end amplitude is Φ_d^0. Although the substrate and the base plate undergo moderate bending with no inflection point, we may use the elastica theory to describe their nonlinear deformation. In this case, the inflection points are outside the actual elastic curve. For a slightly buckled configuration, the amplitude, Φ_d, can be expanded in terms of the distortion parameter of the delaminated layer, ϵ, as follows

$$\Phi_d = \Phi_d^0 + \phi_d^{(1)}\epsilon + \phi_d^{(2)}\epsilon^2 + O(\epsilon^3) \tag{1}$$

The end rotation at the common section, θ, at the critical state is $\theta^0 = 0$. The common section of the configuration is where the delamination starts or ends, that is, where the three parts of the structure meet. The end rotation can be expanded in Taylor series in terms of ϵ. The relevant expression in Ref *24* gives

$$\theta = (\sin \Phi d)\epsilon - \frac{1}{24}(\sin \Phi d \cos^2 \Phi d)\epsilon^3 + \cdots = (\sin \Phi_d^0)\epsilon + (\cos \Phi_d^0)\phi_d^{(1)}\epsilon^2$$

$$+ \left[(\cos \Phi_d^0)\phi_d^{(2)} - (\sin \Phi_d^0)\frac{\phi_d^{(1)2}}{2} - \frac{1}{24}\sin \Phi_d^0 \cos^2 \Phi_d^0\right]\epsilon^3 \tag{2}$$

$$= \theta^{(1)}\epsilon + \theta^{(2)}\epsilon^2 + \theta^{(3)}\epsilon^3 + O(\epsilon^4)$$

At the common section, conditions of geometrical continuity should be fulfilled. Therefore, the end rotation at the common section is the same for the delaminated, the substrate and the base plate.

Similar to the end rotation, θ, the axial force, P_d, the moment, M_d and the flexural contraction, f_d, of the delaminated plate can be expanded in Taylor series in terms of the ϵ, after their substitution in the relevant Britvek's [24] formulas. At the critical state $P_d \equiv P_d^0$ and $M_d \equiv M_d^0 = 0$. For example, the asymptotic expansion of the axial force, P_d, is

$$\frac{\ell^2 P_d}{D_d} = \frac{\ell^2}{D_d}(P_d^0 + P_d^{(1)}\epsilon + P_d^{(2)}\epsilon^2) + O(\epsilon^3) \tag{3}$$

For the substrate plate, the amplitude, Φ_s, and the distortion parameter, α_s, are expanded in terms of the distortion parameter of the delaminated plate, ϵ

$$\Phi_s = \Phi_s^0 + \phi_s^{(1)}\epsilon + \phi_s^{(2)}\epsilon^2 + O(\epsilon^3) \tag{4}$$

$$\alpha_s = \alpha_s^{(1)}\epsilon + \alpha_s^{(2)}\epsilon^2 + \alpha_s^{(3)}\epsilon^3 + O(\epsilon^4) \tag{5}$$

At the common section of the base plate, $\Phi = \Phi_b$. The amplitude and the distortion parameter of the base plate are expanded in terms of the distortion parameter of the delaminated plate, ϵ, in a similar manner as the substrate plate in Eqs 4 and 5.

Furthermore, the axial forces, P_s and P_b, the end moments, M_s and M_b, the flexural contractions, f_s and f_b, of the substrate and the base plate, respectively, along with the end rotation at the common section, θ, can be expanded similarly in Taylor series in terms of ϵ.

The next step in this analysis is the definition of the nonlinear critical path. To do so, conditions of force and moment equilibrium at the common section, along with compatibility of the shortening of the delaminated and substrate plates, are required. These conditions will be imposed in the force and deformation asymptotic expressions separately for the first-, second-, and third-order terms. The system of equations to be solved in order to derive one equation with only the distortion parameter, ϵ, as unknown, includes: (*a*) one nonlinear equation for the zero order terms, which defines the critical point (characteristic equation), (*b*) two linear algebraic equations for $\phi_d^{(1)}$ and $\phi_s^{(1)}$ that determine the first order forces, and (*c*) two linear algebraic equations for $\phi_d^{(2)}$ and $\phi_s^{(2)}$ that determine the second-order forces [12].

Next, the initial postbuckling solution briefly described earlier is used in conjunction with the interface crack solution given by Hutchinson and Suo [26]. This solution for a general bimaterial crack is based on the Dundurs [28] material mismatch parameters, $\tilde{\alpha}$ (a measure of the mismatch in the plane tensile modulus across the interface) and $\tilde{\beta}$ (a measure of the mismatch in the in-plane bulk modulus), and the bimaterial constant, $\tilde{\epsilon}$. For the structure under consideration, the crack grows in the resin content between two plies in the direction of the zero degree plies. Therefore, this case is treated as two isotropic materials joined along the longitudinal axis (loading direction). During growth, the *h*/*T* ratio for each specimen remains constant because the crack grows in the interface between the delaminated and the substrate plates. Delamination branching is not considered in the model. At all times, the crack front is straight and perpendicular to the structure's loading direction. The specimen is loaded symmetrically, and the delamination is placed symmetrically along the article's length. For the type of material, specimen geometry, and type of loading considered in this study, the parameters $\tilde{\alpha}$, $\tilde{\beta}$, and $\tilde{\epsilon}$ are equal to zero. In such case, for the plane-strain interface crack shown in Fig. 1, the energy release rate is given by [26]

$$G = \frac{1 - \sqrt{\nu_{12}\nu_{21}}}{2E_1}\left[\frac{P^{*2}}{Ah} + \frac{M^{*2}}{Ih^3} + 2\frac{P^*M^*}{\sqrt{AIh^2}}\sin\gamma\right] \tag{6}$$

where P^*, M^* are linear combinations of the loads from the previous postbuckling solution

$$P^* = P_d - C_1P - C_2\frac{M_b}{h} \tag{7}$$

$$M^* = M_d - C_3M_b \tag{8}$$

The angle, γ, is constrained such that $\gamma < \pi/2$. Moreover, A and I are positive dimensionless numbers that depend on the dimensions of the configuration.

When $\tilde{\beta} = 0$ the Mode I component of the stress intensity factor, K_I, is the amplitude of the singularity of the normal stresses in front of the crack-tip and the associated normal separation of the crack flanks; the Mode II component of the stress intensity factor, K_{II}, governs the shear stress on the interface and the relative shearing displacement of the flanks. The following expressions describe the Mode I and Mode II stress intensity factors

$$K_I = \frac{1}{\sqrt{2}}\left[\frac{P^*}{\sqrt{Ah}}\cos\omega + \frac{M^*}{\sqrt{Ih^3}}\sin(\omega + \gamma)\right] \tag{9a}$$

and

$$K_{II} = \frac{1}{\sqrt{2}}\left[\frac{P^*}{\sqrt{Ah}}\sin\omega + \frac{M^*}{\sqrt{Ih^3}}\cos(\omega + \gamma)\right] \tag{9b}$$

The stress intensity factors, K_I and K_{II}, are expressed with respect to the linear combinations of the loads given from the initial postbuckling solution, and therefore they are known functions of ω. The accurate determination of ω requires the numerical solution of an integral equation and has been reported by Suo and Hutchinson [25].

The mode mixity expresses the relative amounts of Mode I (opening) and Mode II (shearing) components and is defined by

$$\psi = \tan^{-1}\frac{K_{II}}{K_I} = \tan^{-1}\left[\frac{b\sin\omega - \cos(\omega + \gamma)}{b\cos\omega + \sin(\omega + \gamma)}\right] \tag{10}$$

where b measures the loading combination as

$$b = \sqrt{\frac{I}{A}}\frac{P^*h}{M^*} \tag{10a}$$

In order to obtain the energy release rate, G, and the stress intensity factors, K_I and K_{II}, the results derived from the initial postbuckling solution are employed. The asymptotic expressions for the forces and the moments derived from this solution are

$$P^* = \epsilon P^{*(1)} + \epsilon^2 P^{*(2)} + \cdots \tag{11}$$

$$M^* = \epsilon M^{*(1)} + \epsilon^2 M^{*(2)} + \cdots \tag{12}$$

Notice that the zero-order terms cancel out. More explicitly, the kth order terms, that is, $k = 1, 2$ denote the first- and the second-order terms for the load and the moment as follows

$$P^{*(k)} = \frac{H}{T} P_d^{(k)} - \frac{h}{T} P_s^{(k)} - \frac{6hH}{T^3} M_b^{(k)} \tag{13}$$

$$M^{*(k)} = M_d^{(k)} - \frac{h^3}{T^3} M_b^{(k)} \tag{14}$$

The force and moment quantities on the right hand side of these equations are known from the initial postbuckling solution.

In order to find a closed-form solution, the energy release rate and the stress intensity factors are expressed in an asymptotic form with respect to the distortion parameter, ϵ.

$$G = \epsilon^2 G^{(2)} + \epsilon^3 G^{(3)} + \cdots \tag{15}$$

$$K_{\mathrm{I,II}} = \epsilon K_{\mathrm{I,II}}^{(1)} + \epsilon^2 K_{\mathrm{I,II}}^{(2)} + \cdots \tag{16}$$

The quantity needed to complete the initial postbuckling solution is the applied strain, ϵ_0, that represents the "loading" quantity.

$$\epsilon_0 = \epsilon_0^{(0)} + \epsilon_0^{(1)}\epsilon + \epsilon_0^{(2)}\epsilon^2 \tag{17}$$

with

$$\epsilon_0^{(0)} = \frac{P^0}{ET} \quad \text{and} \quad \epsilon_0^{(1)} = \frac{P^{(1)}b}{ET} + \frac{P_d^{(1)}l}{Eh} + \frac{H}{2}\theta^{(1)}$$

$$\epsilon_0^{(2)} = \frac{f_d^{(2)}}{2} + \frac{P_d^{(2)}l}{Eh} + f_b^{(2)} + \frac{P_d^{(2)}b}{ET} + \frac{H}{2}\theta^{(2)}$$

From the preceding expression for ϵ_0 and the perturbation expressions, the computation of ϵ (distortion parameter) is possible for a given applied displacement. Thereafter, all the load and deformation quantities can be expressed with respect to ϵ and evaluated accordingly.

Cyclic Growth Law

The energy release rate, G, has been used by numerous researchers in order to predict the crack growth. In this respect, a Griffith type of criterion is used for the prediction of crack growth. According to this criterion, the energy release rate, G, is compared with the fracture toughness of the specimen, Γ_0. The growth of the delamination is assured when the following condition exists

$$G(\epsilon_0, \ell) > \Gamma_0 \tag{18}$$

The energy release rate, G, depends only on the length of the delamination, ℓ, and the applied strain, ϵ_0, for the present specimen configuration. The fracture toughness, Γ_0, can be expressed in terms of the Mode I and Mode II stress intensity factors, K_I and K_{II}, respectively [*29,30*].

A brief description of the parameters influencing the crack growth in the area in front of the crack-tip is given in the sequence. Kardomateas [*8*], in his initial postbuckling solution model, showed the dependence of the mode mixity on the applied strain and the position of the delamination inside the specimen. In addition, it was proved that the mode mixity changes as the delamination grows. To support these results, well-correlating experiments on graphite/epoxy unidirectional specimens were conducted [*11*].

The stress field in the area surrounding the crack-tip for a specimen subjected to fatigue is characterized by three parameters that describe its intensity and variation due to loading and geometry configuration. The three parameters are the mode mixity, ψ, the load ratio, α, with $\alpha = G_{min}/G_{max}$, and the variation of the energy release rate from G_{min} to G_{max}. Therefore, the amount of crack extension per cycle of loading can be completely described by these parameters, and in a functional form this will be

$$\frac{da}{dN} = f(G_{max}, \alpha, \psi) \tag{19}$$

The mode dependence of the delamination growth process is not yet fully understood and is a subject of research [*20,31,32*]. O'Brien and Kevin [*32*] examined the stacking sequence effect on the local delamination onset in fatigue loading. In their study, a strain energy release rate solution for a local delamination growing from an angle ply matrix crack was used in order to identify these local delaminations and their fracture mode dependence. The results showed the need for detailed analysis on the delamination fracture modes, and a mixed-mode delamination fatigue onset criteria was demonstrated.

For the time being, let us assume that the fracture toughness, Γ_0, depends on the mode mixity; it is generally increasing when $|\psi|$ is increasing, that is, increasing Mode II component. Then the mode-mixity-adjusted fracture toughness is described by Hutchinson and Suo [*26*] as

$$\Gamma_0(\psi) = G_I^c[1 + (\lambda - 1)\sin^2 \psi]^{-1} \tag{20}$$

where $\lambda = G_I^c/G_{II}^c$.

The values of G_I^c and G_{II}^c are the pure Mode I and Mode II toughness, respectively. The parameter, λ, adjusts the influence of the Mode II contribution in the criterion and should be determined experimentally by obtaining mode interaction curves as in Ref *20*. Notice that for pure Mode I, $\psi = 0$ and $\Gamma_0 = G_I^c$, and for pure Mode II, $\psi = 90^0$ and $\Gamma_0 = G_{II}^c$. A typical value for λ for graphite/epoxy is $\lambda = 0.30$. When $\lambda = 1$ then $G_I^c = \Gamma_0$ for all mode combinations.

In order to include the effect of mode-dependent toughness in the crack growth in the initial postbuckling solution discussed before, we define the mode-adjusted crack driving force, $\tilde{G}$, as follows

$$\tilde{G} = \frac{G}{\Gamma_0(\psi)} = \tilde{G}(\epsilon_0, \psi) \tag{21}$$

For crack advance

$$G/\Gamma_0(\psi) \geq 1 \Leftrightarrow \tilde{G}(\epsilon_0, \psi) \geq 1 \tag{22}$$

To derive the mode mixity, ψ, in a closed-form solution, the postbuckling solution suggested

by Kardomateas [12] was used. This theoretical model assumes cyclic loading from an unloaded position to a maximum compressive strain, ϵ_{max}. Since the stress intensity factors for pure Mode I and II are known, the mode mixity is given by the following equivalent with Eq 10

$$\psi = \tan^{-1} \frac{\epsilon K_{II}^{(1)} + \epsilon^2 K_{II}^{(2)}}{\epsilon K_{I}^{(1)} + \epsilon^2 K_{I}^{(2)}} \tag{23}$$

The stability of the crack growth can be assessed from the study of a energy release rate, G, versus delamination length, ℓ, diagram for a specific applied strain, ϵ_{max}. For the specified strain $\epsilon_0 = E_0$, the corresponding ϵ is determined from the minimum (negative) root of the equation

$$E_0 = \epsilon_0^{(0)}(\ell) + \epsilon_0^{(1)}(\ell)\epsilon + \epsilon_0^{(2)}(\ell)\epsilon^2 \tag{24}$$

Then the corresponding energy release rate, G, is

$$G(\ell) = G^{(2)}(\ell)\epsilon^2 + G^{(3)}(\ell)\epsilon^3 \tag{25}$$

The delamination growth is stable when the $G - \ell$ curve has a negative slope, otherwise the delamination growth is unstable [16].

Based on the preceding discussion, the assumption that slow growth takes place in the interface between the 0 and 90 plies and by applying minimum load close to zero, therefore, load ratio $\alpha = 0$, the following crack growth law is derived

$$\frac{da}{dN} = C(\psi) \frac{(\Delta \tilde{G})^{m(\psi)}}{1 - \tilde{G}_{max}} \tag{26}$$

where $\Delta\tilde{G}$ is the variation mode adjusted crack driving force (variation of the energy release rate normalized with the fracture toughness), $\Delta\tilde{G} = \tilde{G}_{max} - \tilde{G}_{min}$. The $1 - \tilde{G}_{max}$ in the denominator was introduced to account for very short life (less than 10^3 cycles). A similar power growth law is seen in the Paris fatigue law. In contrast, the Paris formulation uses the stress intensity factor, ΔK, for a single pure mode instead of $\Delta\tilde{G}$.

The mode dependency of the $C(\psi)$ and $m(\psi)$ parameters has been demonstrated experimentally by Russell and Street [9]. Although a slightly different growth law was used for graphite/epoxy these parameters were found to be $C_I = 0.0325$ and $m_I = 5.8$ for pure Mode I, and $C_{II} = 0.285$ and $m_{II} = 9.4$ for pure Mode II. The $C(\psi)$ and $m(\psi)$ parameters can be expressed in terms of the mode mixity following the same format as Hutchinson and Suo's [26] formula for the fracture toughness, Γ_0. Therefore, $m(\psi)$ and $C(\psi)$ are described by the following equations, respectively

$$m(\psi) = m_I[1 + (\mu - 1)\sin^2\psi] \tag{27}$$

and

$$C(\psi) = C_I[1 + (\kappa - 1)\sin^2\psi] \tag{28}$$

where μ is defined as the ratio of the exponents, m, at Modes II and I, and κ is defined as the ratio of the constant, C, at Modes II and I. In general, μ is less than 1 and κ is greater than 1. The present experimental study uses values of μ and κ very close to the values that

Russell and Street [9] determined by conducting pure Mode I and II tests for double cantilever beam (DCB) and end-delaminated flexure specimens. Equations 27 and 28 are semi-empirical and characterize the mode dependency of the delamination cyclic growth law.

Experimental Approach

In deriving the cyclic growth law presented in the preceding sections, it was assumed that for a given level of mode mixity, ψ, the parameters that control the rate of the delamination growth are: (*a*) the maximum value of the energy release rate near the tip of the delamination, and (*b*) the variation (spread) energy release rate in the loading/unloading cycle. We validate this assumption by using the growth law to predict the growth rate for the specimen configurations with: (1) different positions of the delamination through the thickness, and (2) different values of the applied maximum external compression, ϵ_{max}. It will be seen that, despite the wide range of combinations, the correlation between experiment and prediction is reasonable. Therefore, from simple laboratory tests, we can use this formulation to predict the number of cycles required for a delamination to grow by a specific amount, and a reliable analysis for the near-tip state of mode mixity and energy release rate can be obtained.

The material used in this study is C30/922 graphite/epoxy. The material was provided in the form of unidirectional prepreg tapes. The elastic constants of the C30/922 graphite/epoxy are: Young's modulus, E_L = 137.90 GPa and E_T = 8.98 GPa in longitudinal and transverse direction respectively; shear modulus, G_{LT} = 7.10 GPa; and in-plane Poisson's ratio, ν_{LT} = 0.30. The thickness of the prepeg tape is 8.89×10^{-5} m (0.0035 in.). The thermoset resin content by weight of C30/922 is 33 ± 3%.

The use of prepeg tapes is advantageous because it allows easy manufacturing of laminates with various ply orientations. In this study, cross-ply specimens are manufactured by hand layup of each ply following the desired stacking sequence. The delamination is introduced in each specimen with a Teflon film insert. A primary concern in the film selection is the film's thickness. Thick insert films can distort the experimental results by introducing resin pockets in front of the crack-tips. Murri and Martin [33] have studied the effect of insert thickness on fracture toughness testing. Their study concludes that inserts of 13×10^{-6} m (0.00051 in.) do not produce resin pockets while inserts of 75×10^{-6} m (0.00295 in.) and thicker do produce resin pockets. The insert is DuPont Teflon FEP film of 2.7×10^{-6} m (0.0005 in.) thickness. Once the delamination is implanted symmetrically along the length of each specimen and the plies are laid up, then the specimens are cured in an autoclave following the manufacturer's standardized curing cycle for C30/922 graphite/epoxy.

The test articles were cut to the desired dimensions: $w = 12.7 \times 10^{-3}$ m (0.5 in.) wide and $\ell = 152.4 \times 10^{-3}$ m (6.0 in.) total length. The free length of the specimen (length measured between the grips) was $2L = 96.5 \times 10^{-3}$ m (3.8 in.). The thickness of the delaminated plate was $h = 0.4 \times 10^{-3}$ m (0.0525 in.). The thickness of the base plates was $T = 1.3 \times 10^{-3}$ m (0.05 in.) for the 4/15 specimen configuration and $T = 2.6 \times 10^{-3}$ m (0.10 in.) for the 4/29 specimen configuration. The thickness measurements were taken after the curing of each specimen, and at eight different locations along its length in order to assure its constant thickness and reveal any geometric distortions.

Monotonic compressive displacement tests were conducted to open the delaminations and release the Teflon inserts. Furthermore, the applied cyclic strain that each specimen was subjected to during fatigue tests was determined based on the displacement level where no further static growth of delamination is observed under static compressive experiments.

The fatigue tests were conducted on cross-ply graphite/epoxy specimens with the aforementioned dimensions in an Instron servohydraulic testing machine. The boundary conditions imposed on each specimen when inserted to the Instron testing machine are clamped-clamped

[*34*]. Monitoring of the delamination growth was conducted with a Questar remote video measurement system that allows tri-axial motion of a microscope and simultaneous digital measurement of distances. The experiments were conducted under 3-Hz frequency and under constant ϵ_{max} (displacement control).

Two specimen configurations were tested. The first one consisted of a total of 15 plies with the delamination positioned between the fourth and the fifth ply. This configuration was tested for two different values of the applied strains, ϵ_{max}. The second configuration consisted of 29 plies with the same delamination position as before, so the same delamination thickness existed in all experiments. Each specimen had the same initial delamination length and was subjected to different applied maximum compressive strains. The cross-ply graphite/epoxy configurations were:

(*a*) 15 plies, delamination of half length, $\ell_0 = 25.4 \times 10^{-3}$ m (1.0 in.); $h/T = 4/15 = 0.2667$; maximum compressive strain, $\epsilon_{max} = 1.579 \times 10^{-3}$, noted as 4/15b.
(*b*) 15 plies, delamination of half length, $\ell_0 = 25.4 \times 10^{-3}$ m (1.0 in.); $h/T = 4/15 = 0.2667$; maximum compressive strain, $\epsilon_{max} = 2.632 \times 10^{-3}$, noted as 4/15c.
(*c*) 29 plies, delamination of half length, $\ell_0 = 25.4 \times 10^{-3}$ m (1.0 in.); $h/T = 4/29 = 0.1379$; maximum compressive strain, $\epsilon_{max} = 1.316 \times 10^{-3}$, noted as 4/29a.

The fatigue growth parameters of the cross-ply graphite/epoxy specimens that were tested were: exponent ratio $\mu = m_{II}/m_I = 0.5$ and constant ratio $\kappa = C_{II}/C_I = 10$. The critical energy release rate for Mode I, that is, Mode I interlaminar fracture toughness, G_I^C, of the cross-ply graphite/epoxy specimens, was determined by static DCB experiments that were conducted according to the standard testing method ASTM Test Method for Mode I for Interlaminar Fracture Toughness of Unidirectional Fiber-Reinforced Polymer Matrix Composites (D 5528-94A). Although the DCB tests have been used extensively and are recommended for unidirectional glass fiber reinforced structures, they can be used for structures with different material, architecture, and layup than the one proposed in the standard method, provided some caution and corrections, if needed, are used. For nonunidirectional configurations, like the cross-ply graphite/epoxy structures discussed in this paper, the values of the observed initiation values of G_I^C established by DCB tests can be affected from one, or both, of the following cases: (1) branching of the delamination away from the midplane through matrix cracks in off-axis plies that results in coupling between extension and shear due to the formation of asymmetric sublaminates as the delamination grows (in such cases pure Mode I fracture is not achieved); and (2) anticlastic bending effects that result in nonuniform delamination growth along the specimen's width. A number of tests was conducted in order to ensure the validity of the results obtained from the DCB tests. The delamination opening and growth was closely monitored and video taped through a Questar tele-microscope. A mirror devise attached to the tele-microscope enabled the observation of the delamination through the width of the specimen. After the completion of each test, each specimen was separated catastrophically along its midplane, and the delamination front was examined to ensure uniform delamination growth along the specimen's width. The method of data reduction used to calculate the G_I^C was the modified beam theory (MTB) that is the one recommended in ASTM D 5528-94A. The value determined was $G_I^C = 200$ N/m. The Mode II interlaminar fracture toughness, G_I^C, was determined by assuming the value of the ratio of Mode I and Mode II interlaminar fracture toughness to be $\lambda = 0.30$, which is a typical value for graphite/epoxy.

Discussion of Results

Experimental Results

The experimental results from the fatigue tests are presented in Fig. 2 as distinct points. The experiments were carried under displacement control, and the cyclic loading was always compressive. In Fig. 2 it is apparent that the two different configurations present different delamination growth behavior. Also, the effect of the applied strain in the 4/30 configuration changes the growth behavior of the delamination. By comparing the 4/15b and 4/15c configurations, it seems, that the higher the applied strain, for example, 4/15c, the faster the delamination growth.

Discussion of the experimental and analytical correlation for the cross-ply graphite/epoxy specimens follows in the next section.

Analytical Results

The theory described earlier will now be applied to the specimen configuration used in experiments. From this operation, the graphical representations of the mode mixity, the energy release rate, as well as the delamination growth versus the number of cycles are derived.

In the present study, we are going to compare the theoretical results obtained from the analysis of the cross-ply specimens with results obtained from the same model but for unidirectional specimens from Ref *11*.

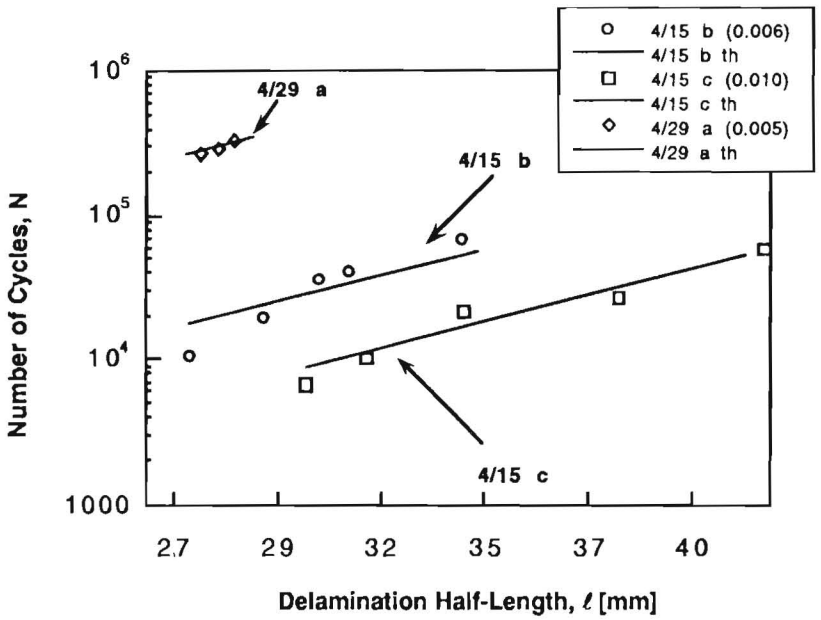

FIG. 2—*Fatigue delamination growth,* N-ℓ *(semilogarithmic plot), for cross-ply specimens. The number in the parenthesis denotes the maximum displacement applied to each specimen (1 in. = 0.0254 m). In each case, the experimental data are denoted with discrete empty marks, whereas the lines represent the predictions of theory. Proposed crack growth law parameters:* $m_I = 4.6$, $C_I = 0.696$ *m/cycle.*

Results from the Cross-Ply Specimens—The mode mixity, ψ and the energy release rate spreads, $\tilde{G}$ that the 4/29a, 4/15b, and 4/15c configurations exhibit are shown in Fig. 3 and Fig. 4, respectively. In Fig. 3, the vertical axis is the mode mixity. As seen at Fig. 3, the mode mixity versus the delamination half-length changes for each specimen configuration. As the delamination grows, the mode mixity reduces giving rise to its Mode II component; pure Mode II is $-90°$. The mode mixity exhibited by the 4/29 specimen is lower than that exhibited by the two 4/15 specimens. The 4/15 specimen with the larger ϵ_{max} has the smallest mode mixity of the two 4/15 specimens, going to pure Mode II ($\psi = 90°$) when delamination half-length equals 3.28×10^{-2} m. From Fig. 3, it is obvious that the mode mixity depends not only on the *h/T* ratio but also on the maximum applied strain, ϵ_{max}.

All the specimens are subjected to less than 15% of the critical energy release rate, $\Gamma_0(\psi)$. From Fig. 4, it can be concluded that the energy release rate is higher for higher *h/T* ratio, that is, the deeper the delamination is in the specimen. All the configurations exhibit reduction of the energy release rate as the delamination length increases during the fatigue tests.

The parameters, m_1 and C_1, for the mode-dependent cyclic growth law were obtained from three data points (ℓ, N) of the 4/15c specimen. The data points used were: 29.972 mm, 5000 cycles; 31.344 mm, 10 000 cycles; and 34.163 mm, 30 000 cycles, see Table 1. The values obtained were $m_1 = 4.6$ and $C_1 = 0.696$ m/cycle.

Based on these values, the theoretical number of cycles has been evaluated for the three specimens. Figure 2 shows the experimental data (distinct points) and the predicted growth behavior (solid lines). This semi-logarithmic diagram shows the good correlation of experimental and predicted results for the 4/15c specimen. Since the 4/15c specimen's data were used

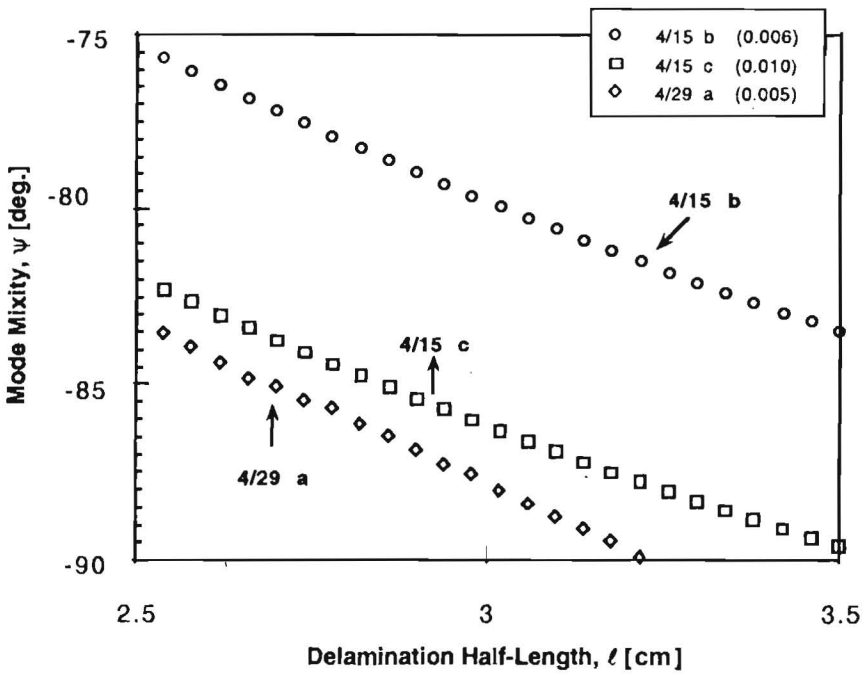

FIG. 3—*Mode mixity, ψ^0 versus delamination half-length, ℓ, for the cross-ply specimen configurations tested. The number in the parenthesis denotes the maximum displacement applied to each specimen (1 in. = 0.0254 m). The pure Mode II is for $\psi = \pm 90^0$.*

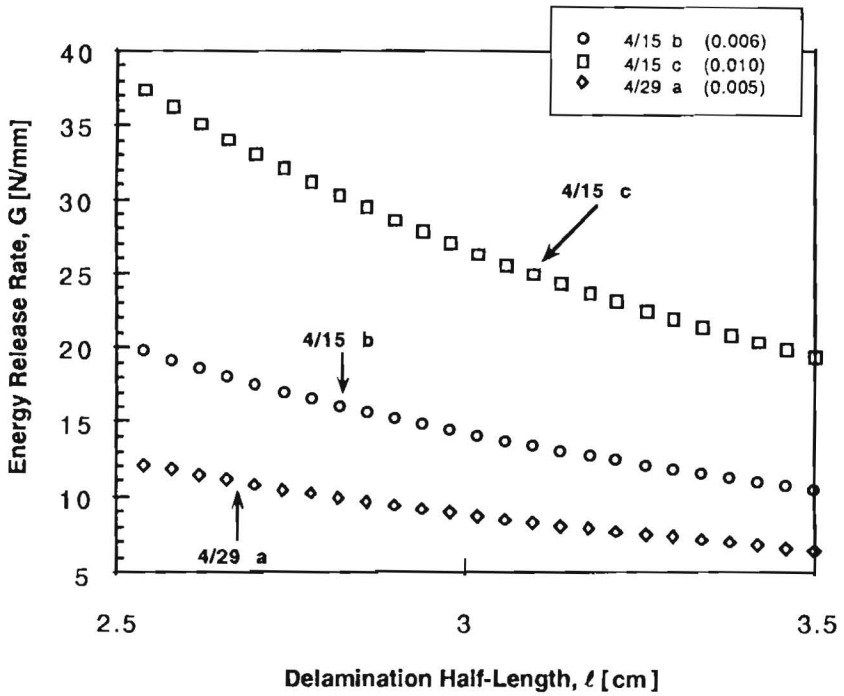

FIG. 4—*Energy release rate, G, versus delamination half-length, ℓ, for the cross-ply specimen configurations tested. The number in the parenthesis denotes the maximum displacement applied to each specimen (1 in. = 0.0254 m).*

TABLE 1—*Comparison with experiments, cross-ply, graphite/epoxy.*

h/T Specimen Type	Delamination Half-Length, mm	*N* Theoretical Cycles, predicted	*N* Experimental Cycles, from tests
4/15b	27.076	15 000	10 426
ℓ_0 = 25.4 mm	31.204	24 979	23 897
T = 1.3 mm	32.423	31 233	33 480
max applied strain = 1.579E-3	33.450	35 374	48 057
4/15c	29.972	5 000	5 000
ℓ_0 = 25.4 mm	31.344	10 003	10 000
T = 1.3 mm	34.163	29 343	30 000
max applied strain = 2.632E-3	41.808	31 246	38 000
4/29a	27.330	281 700	253 503
ℓ_0 = 25.4 mm	27.800	319 940	292 703
T = 2.6 mm	28.207	344 390	329 903
max applied strain = 1.316E-3	28.461	378 640	354 931

[a] G_I^c = 200 N/m; $\lambda = G_I^c/G_{II}^c = 0.30$; $m_I = 4.6$; $C_I = 0.696$ m/cycle; $\mu = m_{II}/m_I = 0.5$; $\kappa = C_{II}/C_I = 10$.

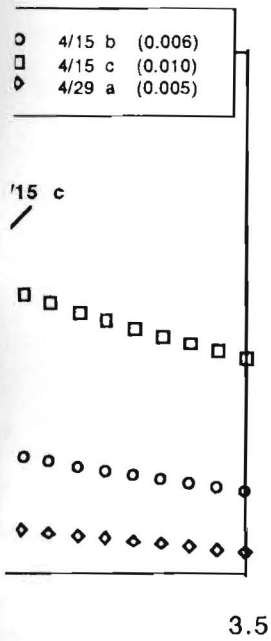

gth, ℓ, for the cross-ply specimen e maximum displacement applied

ly, graphite/epoxy.

N ieoretical Cycles, redicted	*N* Experimental Cycles, from tests
15 000	10 426
24 979	23 897
31 233	33 480
35 374	48 057
5 000	5 000
10 003	10 000
29 343	30 000
31 246	38 000
281 700	253 503
319 940	292 703
344 390	329 903
378 640	354 931

e; $\mu = m_{II}/m_I = 0.5$; $\kappa = C_{II}/C_I = 10$.

to compute m_I and C_I, this behavior was expected. Also, there is reasonable correlation between the experimental and predicted results for specimens 4/15b and 4/29a. The trend to require a higher number of cycles for the delamination growth of specimens with lower *h/T* ratio is apparent. Another observation made from this diagram is that for specimens with the same thickness, that is, same number of plies, the one with the lower initial strain needs a larger number of cycles to exhibit delamination growth.

Comparison Cross-Ply and Unidirectional Configurations—Unidirectional C30/922 graphite/epoxy configurations from Ref *11* are used in order to compare the mode mixity and the energy release rates with the cross-ply configurations of the present study. The unidirectional configurations are 4/15b, 4/15c, and 4/29a. Figure 5 presents the mode mixity versus the delamination half-length for both layups. As seen for all configurations, the mode mixity is higher when the delamination length is smaller. When the delamination opens (increases in length), the mode mixity reduces in favor of the Mode II component. Eventually, 4/15c and 4/29a cross-ply and 4/29a unidirectional reach pure Mode II condition. The trend existing in the cross-ply laminates is the same with the unidirectional ones. The higher the *h/T* ratio in the specimens the higher the Mode I component in the mode mixity. Also, high values of mode mixity are favored in configurations with smaller comparatively applied strain.

The energy release rate comparison is shown in Fig. 6. From this diagram, it is apparent that the values of the energy release rate for the unidirectional specimens are higher than the

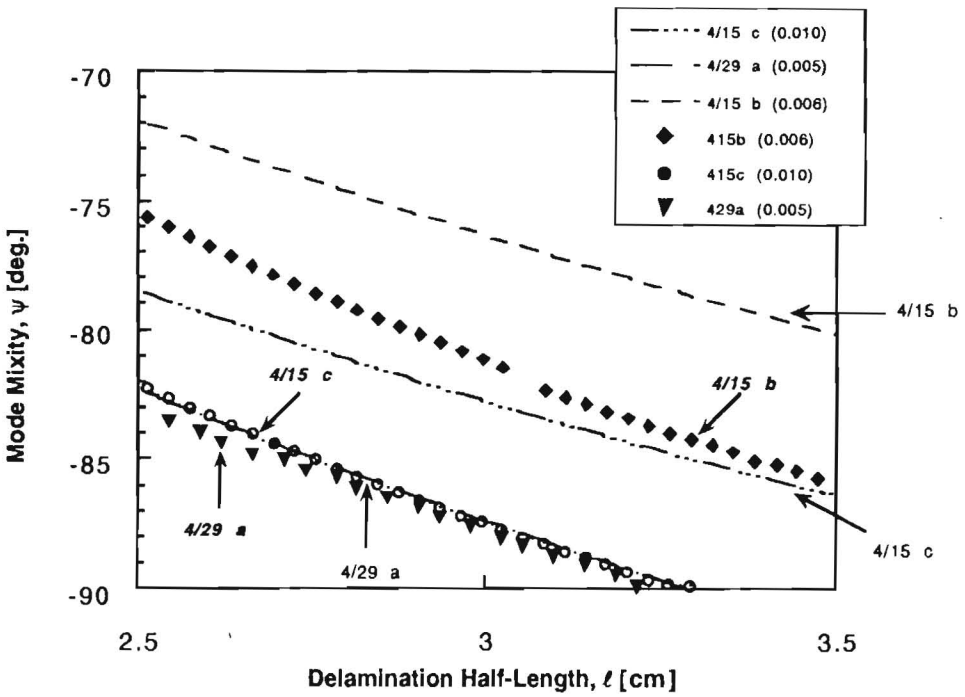

FIG. 5—*Mode mixity, ψ^0, versus delamination half-length, ℓ, for unidirectional specimen configurations (noted by dashed lines) and cross-ply ones (noted by full marks and open circles in the case of 4/15c). The number in the parenthesis denotes the maximum displacement applied to each specimen (1 in. = 0.0254 m). The pure Mode II is for $\psi = \pm 90^0$.*

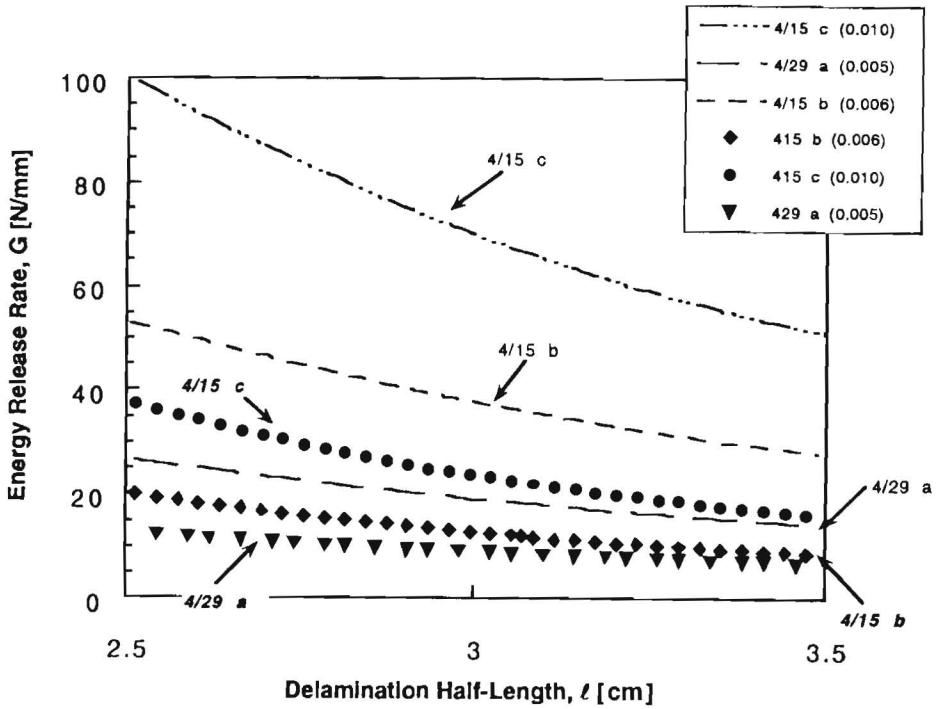

FIG. 6—*Energy release rate, G, versus delamination half-length, ℓ, for unidirectional specimen configurations (noted by dashed lines) and cross-ply ones (noted by full marks). The number in the parenthesis denotes the maximum displacement applied to each specimen (1 in. = 0.0254 m).*

corresponding cross-ply values. For both layups the energy release rate is higher for higher *h/T* ratios with the smaller applied strain. A possible explanation for this trend is given through the initial postbuckling solution model. As seen in this model, the energy release rate is directly analogous to the forces and moments applied at the common cross section at each time. The absolute values of these loads are smaller in the case of the cross-ply specimens.

The plot of the number of cycles versus the delamination length for the unidirectional layup is shown in Fig. 7. The m_I and C_I parameters for the mode-dependent cyclic growth law for the unidirectional specimens were obtained from three data points (ℓ, N) of the 4/30b specimen. The data points used were: 24.130 mm, 86 280 cycles; 24.968 mm, 151 012 cycles; and 25.781 mm, 231 985 cycles. The values obtained were $m_I = 10.385$ and $C_I = 0.0435$ m/cycle.

The experiments made for this case used the 4/30 and 4/15 configurations with different initial strains than the ones used in the cross-ply layup. Therefore, the comparison regarding the growth rate is treated through the proposed crack growth law. From the proposed law, it is concluded that the delamination grows faster in the unidirectional specimens than in the cross-ply ones, since the m_I exponent is larger in the unidirectional case, that is, $m_I = 10.385$ for the unidirectional and $m_I = 4.6$ for the cross-ply specimens. In addition, from Figs. 2 and 7, it is apparent that similar trends relating the number of cycles required to grow the delamination and the *h/T* ratio hold for both specimen types. The number of cycles needed for delamination growth is higher for smaller ratios in both cases. This conclusion comes from the study of the energy release rate diagram. The low *h/T* ratio specimens have a lower energy release rate than the specimens with high *h/T* ratios. Therefore, they require a larger number of cycles

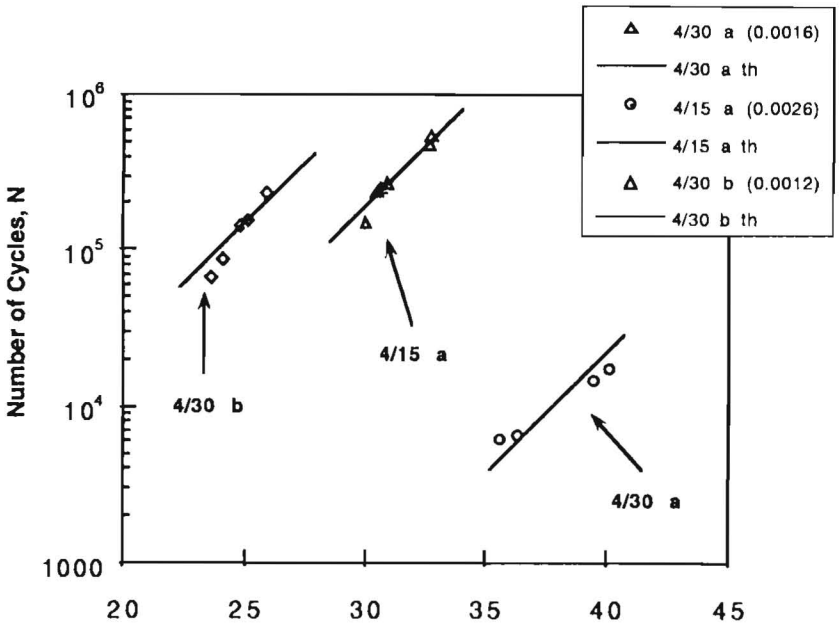

FIG. 7—*Fatigue delamination growth, N-ℓ (semilogarithmic plot), for unidirectional specimens [11]. The number in the parenthesis denotes the initial displacement applied to each specimen (1 in. = 0.0254 m). In each case, the experimental data are denoted with discrete empty marks, whereas the lines represent the predictions of theory. Proposed crack growth law parameters:* m_I *= 10.385,* C_I *= 0.0435 m/cycle.*

to grow the same amount of delamination. Another parameter related to the number of cycles required to grow a delamination is the initial applied strain. Figures 2 and 7 show that the number of cycles required for the same specimen configuration is smaller if the initial strain applied is larger. The unidirectional configurations seem to be more sensitive to this parameter than the cross-ply ones, since for a small difference in the initial strain value the number of cycles required for the 4/30a specimen decreases dramatically.

Conclusions

In this study, C30/922 cross-ply graphite/epoxy configurations are experimentally and analytically examined under compressive fatigue loading at constant displacement amplitude. Delaminations are introduced in the specimens and the effects of applied strain, and delamination length on the energy release rate, mode mixity, and delamination fatigue growth behavior is investigated. The delaminated specimens undergo buckling. The results from the cross-ply specimens of the present study are compared with results of unidirectional specimens from a previous study.

From the tests and the analysis conducted, the following results are summarized:

1. Experimental and analytical results indicate that the number of cycles required for delamination growth is larger for cross-ply specimens than for unidirectional specimens at the same applied maximum strain.

2. Analytical results indicate that the energy release rate reduces with delamination growth for both material configurations.
3. The growth of delaminations takes place under mode-mixity conditions characterized by a relatively low Mode II component in the mode mixity for unidirectional, and a relatively high value of Mode II component for cross-ply configurations. For both specimen configurations, the mode mixity decreases as the delamination grows.
4. From the analysis conducted, it was found that the h/T ratio is an important parameter for the energy release rate and the mode mixity in both materials. The trend appears to be that specimens with higher h/T ratios exhibit higher energy release rate values and higher values of Mode I component in the mode mixity.
5. Finally, the correlation between analytical and experimental results is reasonable. The values for the m_1 and C_1 parameters of the mode-dependent cyclic growth law are in good correlation with values established in previous studies [*9,11*].

Acknowledgments

The financial support of the Office of Naval Research, Ship Structures and Systems Division, S & T Division Grant N00014-91-J-1892, and the interest and encouragement of the grant monitor, Dr. Y. Rajapakse, are both gratefully acknowledged. The authors are also grateful to Prof. R. L. Carlson for useful discussions and comments.

References

[*1*] Kardomateas, G. A. and Schmueser, D. W., "Buckling and Postbuckling of Delaminated Composites under Compressive Loads Including Transverse Shear Effects," *Journal of American Institute of Aeronautics and Astronautics*, Vol. 26, No. 3, 1988, pp. 337–343.

[*2*] Hong, S. and Liu, D., "On the Relationship Between Impact Energy and Delamination Area," *Experimental Mechanics*, Vol. 29, No. 2, 1989, pp. 115–120.

[*3*] Chai, H., Babcock, C. D., and Knauss, W. G., "One Dimensional Modeling of Failure in Laminated Plates by Delamination Buckling," *International Journal of Solids and Structures*, Vol. 17, 1981, pp. 1069–1083.

[*4*] Chai, H. and Babcock, C. D., "Two Dimensional Modeling of Compressive Failure in Delaminated Laminates," *Journal of Composite Materials*, Vol. 19, 1985, pp. 67–97.

[*5*] Evans, A. G. and Hutchinson, J. W., "On the Mechanics of Delamination and Spalling in Compressed Films," *International Journal of Solids and Structures*, Vol. 20, No. 5, 1984, pp. 455–466.

[*6*] Shivakumar, K. N. and Whitcomb, J. D., "Buckling of a Sublaminate in a Quasi-Isotropic Composite Laminate," *Journal of Composite Materials*, Vol. 19, 1985, pp. 2–18.

[*7*] Simitses, G. J., Sallam, S., and Yin, W. L., "Effect on Delamination on Axially Loaded Homogenous Laminated Plates," *Journal of American Institute of Aeronautics and Astronautics*, Vol. 23, No. 9, 1985, pp. 1437–1444.

[*8*] Kardomateas, G. A., "Postbuckling Characteristics in Delaminated Kevlar/Epoxy Laminates: An Experimental Study," *Journal of Composites Technology and Research*, Vol. 12, No. 2, 1990, pp. 85–90.

[*9*] Russell, A. J. and Street, K. N., "Predicting Interlaminar Fatigue Crack Growth Rates in Compressively Loaded Laminates," *Composite Materials: Fatigue and Fracture*, Vol. 2, *ASTM STP 1012*, P. Lagace, Ed., American Society for Testing and Materials, Philadelphia, 1989, pp. 162–178.

[*10*] Whitcomb, J. D., "Strain-Energy Release Rate Analysis of Cyclic Delamination Growth in Compressively Loaded Laminates," *Effects of Defects in Composite Materials, ASTM STP 836*, K. L. Reifsnider, Ed., American Society for Testing and Materials, Philadelphia, 1984, pp. 175–193.

[*11*] Kardomateas, G. A., Pelegri, A. A., and Malik, B., "Growth of Internal Delaminations Under Cyclic Compression in Composite Plates," *Failure Mechanics in Advanced Polymeric Composites, AMD Vol. 196*, Y. T. D. S. Rajapakse and G. A. Kardomateas, Eds., American Society of Mechanical Engineers, 1994; *Journal of the Mechanics and Physics of Solids*, Vol. 43, No. 6, 1995, pp. 847–868.

[*12*] Kardomateas, G. A., "The Initial Postbuckling and Growth Behavior of Internal Delaminations in Composite Plates," *Journal of Applied Mechanics*, Vol. 60, 1993, pp. 903–910.

[13] Kardomateas, G. A., "Large Deformation Effects in the Postbuckling Behavior of Composites with Thin Delaminations," *Journal of American Institute of Aeronautics and Astronautics*, Vol. 27, 1989a, pp. 624–631.

[14] Wang, S. S., Zahlan, N. M., and Suemasu, H., "Compressive Stability of Delaminated Random Short Fiber Composites, Part I—Modeling and Methods of Analysis," *Journal of Composite Materials*, Vol. 19, 1985, pp. 296–316.

[15] Sheinman, I. and Adan, M., "The Effect of Shear Deformation on Postbuckling Behavior in Laminated Beams," *Journal of Applied Mechanics*, Vol. 54, 1985, pp. 558–562.

[16] Kardomateas, G. A. and Pelegri, A. A., "The Stability of Delamination Growth in Compressively Loaded Composite Plates," *International Journal of Fracture*, Vol. 65, No. 3, Feb. 1994, pp. 261–276.

[17] Whitcomb, J. D., "Parametric Analytical Study of Instability-Related Delamination Growth," *Composite Science and Technology*, Vol. 25, 1986, pp. 19–48.

[18] Rothschilds, R. J., Gillespie, J. W., Jr., and Carlsson, L. A., "Instability-Related Delamination Growth in Thermoset and Thermoplastic Composites," *Composite Materials: Testing and Design (Eighth Conference), ASTM STP 972*, J. D. Whitcomb, Ed., American Society for Testing and Materials, Philadelphia, 1988, pp. 161–179.

[19] Yin, W. L., "Axisymmetric Buckling and Growth of a Circular Delamination in a Compresses Laminate," *International Journal of Solids and Structures*, Vol. 21, No. 5, 1985, pp. 503–514.

[20] Chai, H., "Experimental Evaluation of Mixed Mode Fracture in Adhesive Bonds," *Experimental Mechanics*, Dec. 1992, pp. 296–303.

[21] O'Brien, T. K., "Towards a Damage Tolerance Philosophy for Composite Materials and Structures," *Composite Materials: Testing and Design, Ninth Volume, ASTM STP 1059*, S. P. Garbo, Ed., American Society for Testing and Materials, Philadelphia, 1990, pp. 7–33.

[22] Sheinman, I. and Kardomateas, G. A., "Energy Release Rate and Stress Intensity Factors for Delaminated Composites," *International Journal of Solids and Structures*, in print.

[23] Sheinman, I., Kardomateas, G. A., and Pelegri, A. A., "Delamination Growth During Pre- and Post-Buckling Phases of Delaminated Composite Laminates," *International Journal of Solids and Structures*, submitted for publication.

[24] Britvek, S. J., The Stability of Elastic Systems, Pergamon, New York, 1973.

[25] Suo, Z. and Hutchinson, J. W., "Interface Crack between Two Elastic Layers," *International Journal of Fracture*, Vol. 43, 1990, pp. 1–18.

[26] Hutchinson, J. W. and Suo, Z., "Mixed Mode Cracking in Layered Materials," *Advances in Applied Mechanics*, Academic Press, New York, Vol. 29, 1992, pp. 63–191.

[27] Agarwal, B. D. and Broutman, L. J., Analysis and Performance of Fiber Composites, 2nd ed., Wiley Interscience, New York, 1990.

[28] Dundurs, J., Mathematical Theory of Dislocations, American Society of Mechanical Engineering, New York, 1969, pp. 70–115.

[29] Suo, Z., "Delamination Specimen for Orthotropic Materials," *Journal of Applied Mechanics: Transactions, American Society of Mechanical Engineers*, Vol. 57, No. 3, Sept. 1990, pp. 627–634.

[30] Hellan, K., Introduction to Fracture Mechanics, Mc Graw Hill, New York, 1984.

[31] Hong, C. S., and Jeong, K. Y., "Stress Intensity Factor in Anisotropic Sandwich Plate with a Part Through Crack Under Mixed Mode Deformation," *Engineering Fracture Mechanics*, Vol. 21, No. 2, 1985, pp. 285–292.

[32] O'Brien, T. K. and Kevin, T., "Mixed-Mode Strain-Energy-Release Rate Effects on Edge Delamination Composites," *Effects of Defects in Composite Materials, ASTM STP 836*, K. L. Reifsnider, Ed., American Society for Testing and Materials, Philadelphia, 1984, pp. 125–142.

[33] Murri, G. B. and Martin, R. H., "Effect of Initial Delamination on Mode I and Mode II Interlaminar Fracture Toughness and Fatigue Threshold," *Composite Materials: Fatigue and Fracture, Fourth Volume, ASTM STP 1156*, W. W. Stinchcomb and N. E. Ashbaugh, Eds., American Society for Testing and Materials, Philadelphia, 1993, pp. 239–256.

[34] Kardomateas, G. A. and Pelegri, A. A., "Growth Behavior of Internal Delaminations in Composite Beam/Plates Under Compression: Effect of the End Conditions," *International Journal of Fracture*, Vol. 75, 1996, pp. 49–67.